

FIG. 1. Graph representing the nonrigid intramolecular rearrangement of the  $C_2H_3^+$  cation.

in the  $LiBH_4$  molecule, according to *ab initio* calculations,<sup>9</sup> the  $Li^+$  cation moves with a small barrier around the  $BH_4^-$  anion, although the anion is a quite stable autonomous unit with very high barriers to its own internal rearrangements. A graph representing the nonrigid intramolecular rearrangements of this species is presented in Fig. 2. The fact that the energetically accessible paths do *not* connect all global minima on the PES of  $LiBH_4$  is shown by the fact

that the graph splits into two subgraphs which differ in the arrangement of the H atoms within the  $BH_4^-$  moiety. The vibrational energy levels of this system will split due to tunneling of the nuclear density function from one minimum to the others, but the splitting pattern will be different than if the  $BH_4^-$  anion were also floppy enough to permit the four H atoms to be exchanged by energetically accessible paths. Such splittings have not yet been found in recent experiments<sup>10</sup> on  $LiBH_4$ , we believe that for analogous molecules in which the energy barriers are smaller (for example,  $LiAlH_4$  has lower barriers than  $LiBH_4$ ), the tunneling splittings will be observable.

Several important questions arise when considering the kind of multim minima structure of potential energy surfaces introduced above. The first question is how to calculate the number of equivalent global minima. The second is how to characterize the nonrigid symmetry. It is clear from the examples discussed above that this symmetry may be obtained from the graph describing the flexible intramolecular rearrangement. The third question involves how to find the symmetry when the graph describing the flexible rearrangements is not connected but is split into two or more equivalent subgraphs. The number of ways a graph may split into subgraphs is also considered in this work. Let us now move on to introduce the group theoretical tools needed to effect the symmetry analysis motivated by the above example.

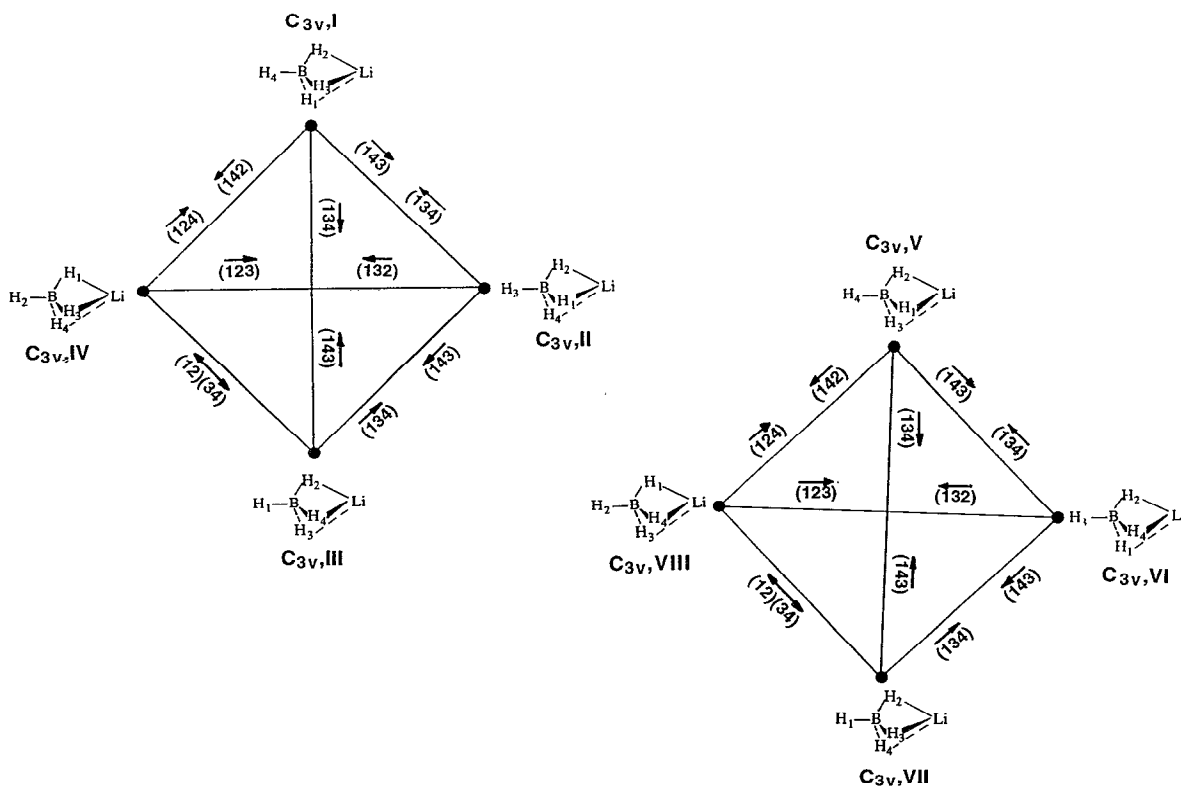


FIG. 2. Graph representing the nonrigid intramolecular rearrangement of the  $LiBH_4$  molecule.

### III. MULTIMINIMA STRUCTURE OF THE POTENTIAL ENERGY SURFACES OF POLYATOMIC MOLECULES

Let us first consider why polyatomic molecules have many global minima and how to calculate the number ( $n$ ) of such minima. Potential energy surfaces arise in the adiabatic approximation to the full Schrödinger equation of the nuclei and electrons when the motions of the nuclei and the electrons are separated. This point of view requires that all of the atomic nuclei are enumerated. Any rearrangement of identical nuclei leads to a new, energetically equivalent, global minimum that corresponds to a distinct geometrical configuration when viewed from this labeled-nuclei point of view. To count the number of such global minima, one has to enumerate the geometries using all permutations, inversions, and permutation-inversions of the equivalent nuclei, excluding those configurations which may be interconverted by either translation or rotation of a rigid geometrical configuration.

For complex polyatomic molecules this is not a simple problem, but there is a very simple rule for counting the number of global minima on the PES of any molecule.<sup>11,12</sup> The number ( $n$ ) of global minima on the PES is equal to the quotient obtained when the order ( $N$ ) of the full permutation-inversion group of that molecule is divided by the order ( $g$ ) of the point group of each rigid global-minimum configuration. The FPI group  $G^{(N)}$  of the molecule represented by the brutto formula  $A_l B_m C_k$  is a direct product of the permutation groups of the identical nuclei and the inversion group  $\epsilon$  (whose order is 2),

$$G^{(N)} = S_l \otimes S_m \otimes S_k \otimes \epsilon,$$

where  $S_l$ ,  $S_m$ ,  $S_k$ , are the groups of permutations of the  $l$ ,  $m$ ,  $k$ , nuclei of types  $A$ ,  $B$ ,  $C$ , respectively. The order of the FPI is thus equal to  $l! \times m! \times k! \times 2$ . For example, for

$$\text{NH}_3, 1! \times 3! \times 2 = 12 = n;$$

$$\text{C}_2\text{H}_6, 2! \times 6! \times 2 = 2880 = n;$$

$$\text{C}_6\text{H}_6, 6! \times 6! \times 2 = 1\,036\,800 = n.$$

The order of the point groups of the rigid global-minimum configurations of  $\text{NH}_3$ ,  $\text{C}_2\text{H}_6$ , and  $\text{C}_6\text{H}_6$  are 6 ( $C_{3v}$ ), 12 ( $D_{3d}$ ), and 24 ( $D_{6h}$ ), respectively. Hence, according to the rule stated above, it can be established that the molecules  $\text{NH}_3$ ,  $\text{C}_2\text{H}_6$ , and  $\text{C}_6\text{H}_6$  have  $12/6=2$ ,  $2880/12=240$ , and  $1\,036\,800/24=43\,200$  energy-equivalent global minima on their PESs.

These data form the first piece of information needed to implement the tools treated in this paper, the number of vertices ( $n$ ) to draw in the graph. Whether a given vertex is connected to another vertex by a line segment depends on whether the corresponding minima can be interconverted via an energetically accessible path; this can only be known as a result of experimental spectroscopic or dynamical measurement or quantum chemistry calculation.

### IV. GRAPHICAL REPRESENTATIONS OF POTENTIAL ENERGY SURFACES

Potential energy surfaces of polyatomic molecules are highly multidimensional. It is therefore very useful to find simple graphical representations of PES that take into account all minima that can be connected by flexible intramolecular rearrangements. Graphs<sup>13</sup> are the simplest way to present such attributes with the absolute minima denoted by *vertices* of the graph and the minimum-energy paths shown as the edges (if the energy barrier separating the two minima is too high to be accessible, there is no edge connecting these two minima). Such graphs can have high symmetry since all vertices have the same order (i.e., number of edge lines leading to them), and equivalent minima have geometrical structures that differ only by numeration of the atoms.

In this article, we will consider only cases in which one type of flexible rearrangement connecting equivalent structures is available, although there do exist cases in which two or more accessible paths can interconnect equivalent structures. In our case, single lines can be used to connect pairs of vertices, and only two types of graphs are possible. The first is a *connected graph* describing rearrangements that can connect all global minima to all others; in these graphs all vertices can be reached by moving along edges to all other vertices. The second graphs are *disconnected* and are *split* into two or more disjoint subgraphs. In this case, some vertices cannot be reached from others by moving along edges. The latter apply when energetically accessible nonrigid rearrangements connect only a subset of the global minima on the potential energy surface. Let us consider these two cases separately.

#### A. Potential energy surfaces with connected graphs

If the graph representing a potential energy surface is connected, all of the equivalent global minima are accessible from one another and hence, the nonrigid group of the molecule is its FPI group. Let us consider two examples: the PES of the flexible intramolecular rearrangements of  $\text{ArH}_3^+$  (Fig. 3) and of  $\text{C}_2\text{H}_3^+$  (Fig. 1).

##### 1. $\text{ArH}_3^+$

From the literature,<sup>14</sup> we know that  $\text{ArH}_3^+$  has  $C_{2v}$  symmetry at its three equivalent global-minimum structures, in which the Ar atom is coordinated to an edge of the  $\text{H}_3^+$  triangle. The saddle points connecting these three minima also have  $C_{2v}$  symmetry with the Ar coordinated to a vertex of the  $\text{H}_3^+$  triangle.<sup>14(a)</sup> The graph describing the flexible intramolecular rearrangement is shown in Fig. 3.

We now demonstrate how to identify the applicable nonrigid symmetry group from Fig. 3 and the molecular formula  $\text{ArH}_3^+$ . All three minima have  $C_{2v}$  local symmetry. Starting with the structure  $C_{2v}$ , I in the first global minimum, we note that there are *four elements* in this  $C_{2v}$  local symmetry group. These elements may be represented through the permutation-inversion operations as  $E$ , (23),  $E^*$ , and (23)\*, where  $E$  is the identity operation,  $(ab)$  represents the pairwise interchange of protons  $a$  and  $b$ , and

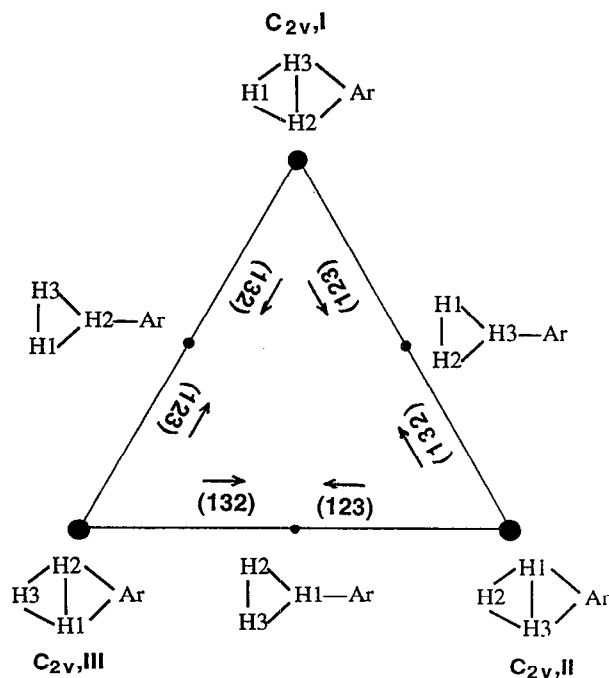


FIG. 3. Graph representing the nonrigid intramolecular rearrangement of the  $\text{ArH}_3^+$  cation.

the \* means *also* invert all particles through to origin. These elements form the first part of the nonrigid group. Next, we introduce the cyclic permutation (123) that leads from the structure  $C_{2v}$ , I into the  $C_{2v}$ , II structure and transfers the molecule from global minimum I into minimum II (see Fig. 3). Here (123) labels the cyclic permutation of the protons in the  $\text{ArH}_3^+$  cation. Next,  $E$ , (23),  $E^*$ , and (23)\* are multiplied by (123) to generate the second set of elements of the nonrigid group. Doing so gives four new elements (123), (12), (123)\*, and (12)\*.

Similarly, (132) transfers structure  $C_{2v}$ , I into  $C_{2v}$ , III. Again, the direct product of  $E$ , (23),  $E^*$ , and (23)\* with (132) gives four new elements: (132), (13), (132)\*, and (13)\*. The final twelve elements:  $E, E^*$ , (12), (12)\*, (13), (13)\*, (23), (23)\*, (123), (123)\*, (132), and (132)\* form the nonrigid group which describes the symmetry of this flexible potential energy surface. This is exactly the full permutation-inversion (FPI) group of the  $\text{ArH}_3^+$  cation, which is the direct product of  $S_3 \otimes S_1 \otimes \epsilon$  and has order  $3! \times 1! \times 2 = N$  (i.e.,  $G^{(12)}$ ). This  $G^{(12)}$  group is isomorphic to the  $D_{3h}$  point group and the table of characters of this group is given in Table I.

According to high level *ab initio* data, this molecule has a very low barrier (3.9 kcal/mol) for intramolecular rearrangement.<sup>14(a)</sup> The high symmetry  $G^{(12)}$  of this floppy system should be observable due to tunneling of its nuclear wave function density from one minimum into another. Indeed, such experimental tunneling splittings in  $\text{ArH}_3^+$  and  $\text{ArD}_3^+$  have been observed by high resolution submillimeter wave spectroscopy.<sup>14(c),14(d)</sup>

TABLE I. Table of characters of the nonrigid  $G^{(12)}$  group of the  $\text{ArH}_3^+$ .

$G^{(12)}$	$E$	(123)	(12)	$E^*$	(123)*	(12)*
Order	1	2	3	1	2	3
$A_1^+$	1	1	1	1	1	1
$A_2^+$	1	1	-1	1	1	-1
$E^+$	2	-1	0	2	-1	0
$A_1^-$	1	1	1	-1	-1	-1
$A_2^-$	1	1	-1	-1	-1	1
$E^-$	2	-1	0	-2	1	0

## 2. $C_2H_3^+$

We have already mentioned in Sec. I that the  $C_2H_3^+$  cation has a bridged global-minimum structure and that its potential energy surface is very flat. The FPI group of this cation is the direct product of the permutational groups  $S_2 \otimes S_3 \otimes \epsilon$ , where  $S_2$  and  $S_3$  are the permutation groups of the carbons and hydrogens, respectively. The order of this group is  $2! \times 3! \times 2 = 24$ . Therefore the number of global minima on the PES calculated according to the rule from the previous section is  $24$  (order of the FPI)/4 (order of  $C_{2v}$ ) = 6.

The graph representing the flexible intramolecular rearrangement of  $C_2H_3^+$  is shown in Fig. 1. This graph is connected and therefore the FPI group is the nonrigid symmetry group of  $C_2H_3^+$  (as well as the  $\text{Be}_2\text{H}_3^-$  anion) which are known<sup>6-8,15</sup> to be flexible molecular systems. The nonrigid group describing the symmetry of the vibration/rotation states of  $C_2H_3^+$  may be obtained from the graph on Fig. 1 and the  $C_{2v}$  local symmetry group. In this case, we have six local  $C_{2v}$  groups. Starting from any global minimum structure [let us take the  $C_{2v}$ , I structure with the four  $E$ , (23)(45),  $E^*$  and (23)(45)\* elements of the local symmetry group], we multiply these four elements by (13)\* which connects  $C_{2v}$ , I and the structure  $C_{2v}$ , II. Moving along the graph in a manner analogous to that detailed above for  $\text{ArH}_3^+$ , we obtain 24 permutation-inversion elements which form the nonrigid group of  $C_2H_3^+$ . This group is exactly the FPI group of this cation and is isomorphic with the  $D_{6h}$  point group; its table of characters is given in Table II [see Ref. 7(a)].

## C. Short cuts

Based on the two examples treated above, one might wonder how the symmetry group of the graph detailing the  $n$  interconnected minima relates to the nonrigid symmetry group of the nonrigid molecule whose PES is represented by the graph. In these two cases above, the graphs  $\text{Gr}(3,2)$  and  $\text{Gr}(6,2)$  (the first integer is the number of connected global minima and the second is the number of minimal energy pathways leading to each minimum) have  $D_3$  and  $D_6$  symmetry.<sup>13</sup> The nonrigid symmetries of  $\text{ArH}_3^+$  and  $C_2H_3^+$  are  $D_{3h}$  and  $D_{6h}$ . Therefore, for molecules whose PES are represented by graphs with  $D_n$  symmetry, the FPI group is the direct product of  $D_n$  and the inversion group:  $D_n \otimes \epsilon$ . The tables of characters of the resulting  $D_{nh}$  groups

TABLE II. Table of characters of the nonrigid  $G^{(24)}$  group of the  $C_2H_3^+$  cation.

	$E$	(123) (45)	(123)	(45)	(12)	(12) (45)	$E^*$	(123) (45)*	(123)*	(45)*	(12)*	(12) (45)*
Order	1	2	2	1	3	3	1	2	2	1	3	3
$A_{1g}^+$	1	1	1	1	1	1	1	1	1	1	1	1
$A_{2g}^+$	1	1	1	1	-1	-1	1	1	1	1	-1	-1
$A_{1u}^+$	1	-1	1	-1	1	-1	1	-1	1	-1	1	-1
$A_{2u}^+$	1	-1	1	-1	-1	1	1	-1	1	-1	-1	1
$E_g^+$	2	-1	-1	2	0	0	2	-1	-1	2	0	0
$E_u^+$	2	1	-1	-2	0	0	2	1	-1	-2	0	0
$A_{1g}^-$	1	1	1	1	1	1	-1	-1	-1	-1	-1	-1
$A_{2g}^-$	1	1	1	1	-1	-1	-1	-1	-1	-1	1	1
$A_{1u}^-$	1	-1	1	-1	1	-1	-1	1	-1	1	-1	1
$A_{2u}^-$	1	-1	1	-1	-1	1	-1	1	-1	1	1	-1
$E_g^-$	2	-1	-1	2	0	0	-2	1	1	-2	0	0
$E_u^-$	2	1	-1	-2	0	0	-2	-1	1	2	0	0

are known and may be used for classification of the vibration/rotation states of such nonrigid species.

Another type of graph whose symmetry generates the nonrigid group of the corresponding molecules is  $Gr(n, n-1)$ . From graph theory<sup>13</sup> it is known that graphs of the form  $Gr(n, n-1)$  have  $S_n$  symmetry. However, molecules that have PES described by  $Gr(n, n-1)$  graphs have higher symmetry than  $S_n$ ; in particular, the FPI groups of molecules having  $Gr(n, n-1)$  graphs are direct products of  $S_n$  and the inversion group:  $S_n \otimes \epsilon$ .

Although these shortcuts can be used for  $Gr(n, n-1)$  and  $Gr(n, 2)$ , in a general case the group of the graph may not relate directly to the nonrigid group of the molecule. Therefore, the tools described above in Secs. IV A 1 and IV A 2 should be used to find all elements of the flexible group starting from the local symmetry elements of the global minimum structure and multiplying by permutation-inversion elements that transfer one structure into another.

#### D. Potential energy surfaces with disconnected graphs

If a graph is used to represent the PES of a species in which high barriers do not allow all of the minima to be reached from *all* other global minima (which is the most common case in floppy molecules), the graph splits into a number of subgraphs (all of which are equivalent). The symmetry obtained from the subgraph then is what determines the symmetry of the vibration/rotation wave functions.

One must know how to form and characterize such subgraphs. Graph theory can solve this problem if the absolute minimum and the transition states connecting them are known, since this information determines the degree of the graph vertices (all of which are equivalent). The order of the vertices is given by the number of minimum energy paths originating in a given absolute minimum and connecting to neighboring minima.

For each graph  $Gr(n, v)$  where  $n$  is the number of vertices and  $v$  is the order of each vertex, one may determine the number ( $k$ ) of subgraphs the original graph can split into. For the initial graph  $Gr(n, v)$  to split into  $k$  equivalent subgraphs (each of which is characterized by  $n_1$  vertices or order  $v$ ), the following conditions have to be satisfied:

$$n = k \times n_1, \quad (1)$$

$$v \leq n_1 - 1, \quad (2)$$

$$q \text{ is } k\text{-fold}, \quad (3)$$

where  $q$  is the number of edges of the graph  $G(n, v)$ .

The first condition requires that the number of vertices in the initial graph  $Gr(n, v)$  and in the  $k$  subgraph  $Gr(n_1, v)$  does not change after splitting; that is, there are  $n$  global minima whether they can or cannot be connected by energetically accessible paths. The second condition points to the fact that the order of the vertex can not be higher than the number of vertices minus 1; that is, each minimum is connected to no more than  $n_1 - 1$  others. The third condition satisfies the Euler theorem for the subgraph  $Gr(n_1, v)$ ,

$$n_1 \times v = 2q. \quad (4)$$

For small values of  $n$  and  $v$ , finding values of  $k$  and  $n_1$  that satisfy conditions (1)–(3) can be checked without utilizing computational devices, but for large values it is difficult, so we have developed a computer program that determines all possible splittings of a graph  $Gr(n, v)$  into  $k$  connected subgraphs  $Gr(n_1, v)$  with  $n_1$  vertices. Table III presents the results of the application of this program to graphs for  $n=6-30$  and  $v=2, 14$ .

To help clarify, let us consider again the  $LiBH_4$  molecule. This molecule was predicted more than 16 years<sup>9</sup> ago to have a very flat potential energy surface with global minima of  $C_{3v}$  symmetry (with the  $Li^+$  cation coordinated to a face of the  $BH_4^-$  tetrahedron). This structure of the global minima was recently experimentally verified.<sup>10</sup> The

TABLE III. All possible splittings of the graphs  $\text{Gr}(n,v)$  into connected subgraphs, where  $n=6-30$  and  $v=2-14$ .<sup>a</sup>

$\text{Gr}(6,2)$ split into 2 $\text{Gr}(3,2)$	$\text{Gr}(8,4)$ split into 2 $\text{Gr}(4,2)$	$\text{Gr}(8,3)$ split into 2 $\text{Gr}(4,3)$	$\text{Gr}(9,3)$ split into 3 $\text{Gr}(3,2)$	$\text{Gr}(10,2)$ split into 2 $\text{Gr}(5,2)$
$\text{Gr}(10,4)$ split into 2 $\text{Gr}(5,4)$	$\text{Gr}(12,2)$ split into 2 $\text{Gr}(6,2)$ or 3 $\text{Gr}(4,2)$ or 4 $\text{Gr}(3,2)$	$\text{Gr}(12,3)$ split into 2 $\text{Gr}(6,3)$ or 3 $\text{Gr}(4,3)$	$\text{Gr}(12,4)$ split into 2 $\text{Gr}(6,4)$	$\text{Gr}(12,5)$ split into 2 $\text{Gr}(6,5)$
$\text{Gr}(14,2)$ split into 2 $\text{Gr}(7,2)$	$\text{Gr}(14,4)$ split into 2 $\text{Gr}(7,4)$	$\text{Gr}(14,6)$ split into 2 $\text{Gr}(7,6)$	$\text{Gr}(15,2)$ split into 3 $\text{Gr}(5,2)$ or 5 $\text{Gr}(3,2)$	$\text{Gr}(15,4)$ split into 3 $\text{Gr}(5,4)$
$\text{Gr}(16,2)$ split into 2 $\text{Gr}(8,2)$ or 4 $\text{Gr}(4,2)$	$\text{Gr}(16,3)$ split into 2 $\text{Gr}(8,3)$ or 4 $\text{Gr}(4,3)$	$\text{Gr}(16,4)$ split into 2 $\text{Gr}(8,4)$	$\text{Gr}(16,5)$ split into 2 $\text{Gr}(8,5)$	$\text{Gr}(16,6)$ split into 2 $\text{Gr}(8,6)$
$\text{Gr}(16,7)$ split into 2 $\text{Gr}(8,7)$	$\text{Gr}(18,2)$ split into 2 $\text{Gr}(9,2)$ or 3 $\text{Gr}(6,2)$ or 6 $\text{Gr}(3,2)$	$\text{Gr}(18,3)$ split into 3 $\text{Gr}(6,3)$	$\text{Gr}(18,4)$ split into 2 $\text{Gr}(9,4)$ or 3 $\text{Gr}(6,4)$	$\text{Gr}(18,5)$ split into 3 $\text{Gr}(6,5)$
$\text{Gr}(18,6)$ split into 2 $\text{Gr}(9,6)$	$\text{Gr}(18,8)$ split into 2 $\text{Gr}(9,8)$	$\text{Gr}(20,2)$ split into 2 $\text{Gr}(10,2)$ or 4 $\text{Gr}(5,2)$ or 5 $\text{Gr}(4,2)$	$\text{Gr}(20,3)$ split into 2 $\text{Gr}(10,3)$ or 5 $\text{Gr}(4,3)$	$\text{Gr}(20,4)$ split into 2 $\text{Gr}(10,4)$ or 4 $\text{Gr}(5,4)$
$\text{Gr}(20,5)$ split into 2 $\text{Gr}(10,5)$	$\text{Gr}(20,6)$ split into 2 $\text{Gr}(10,6)$	$\text{Gr}(20,7)$ split into 2 $\text{Gr}(10,7)$	$\text{Gr}(20,8)$ split into 2 $\text{Gr}(10,8)$	$\text{Gr}(20,9)$ split into 2 $\text{Gr}(10,9)$
$\text{Gr}(21,2)$ split into 3 $\text{Gr}(7,2)$ or 7 $\text{Gr}(3,2)$	$\text{Gr}(21,4)$ split into 3 $\text{Gr}(7,4)$	$\text{Gr}(21,6)$ split into 3 $\text{Gr}(7,6)$	$\text{Gr}(22,2)$ split into 2 $\text{Gr}(11,2)$	$\text{Gr}(22,4)$ split into 2 $\text{Gr}(11,2)$
$\text{Gr}(22,6)$ split into 2 $\text{Gr}(11,6)$	$\text{Gr}(22,8)$ split into 2 $\text{Gr}(11,8)$	$\text{Gr}(22,10)$ split into 2 $\text{Gr}(11,10)$	$\text{Gr}(24,2)$ split into 2 $\text{Gr}(12,2)$ or 3 $\text{Gr}(8,2)$ or 4 $\text{Gr}(6,2)$ or 6 $\text{Gr}(4,2)$ or 8 $\text{Gr}(3,2)$	$\text{Gr}(24,3)$ split into 2 $\text{Gr}(12,3)$ or 3 $\text{Gr}(8,3)$ or 4 $\text{Gr}(6,3)$ or 6 $\text{Gr}(4,3)$
$\text{Gr}(24,4)$ split into 2 $\text{Gr}(12,4)$ or 3 $\text{Gr}(8,4)$ or 4 $\text{Gr}(6,4)$	$\text{Gr}(24,5)$ split into 2 $\text{Gr}(12,5)$ or 3 $\text{Gr}(8,5)$ or 4 $\text{Gr}(6,5)$	$\text{Gr}(24,6)$ split into 2 $\text{Gr}(12,6)$ or 3 $\text{Gr}(8,6)$	$\text{Gr}(24,7)$ split into 2 $\text{Gr}(12,7)$ or 3 $\text{Gr}(8,7)$	$\text{Gr}(24,8)$ split into 2 $\text{Gr}(12,8)$
$\text{Gr}(24,9)$ split into 2 $\text{Gr}(12,9)$	$\text{Gr}(24,10)$ split into 2 $\text{Gr}(12,10)$	$\text{Gr}(24,11)$ split into 2 $\text{Gr}(12,11)$	$\text{Gr}(25,2)$ split into 5 $\text{Gr}(5,2)$	$\text{Gr}(25,4)$ split into 5 $\text{Gr}(5,4)$
$\text{Gr}(26,2)$ split into 2 $\text{Gr}(13,2)$	$\text{Gr}(26,4)$ split into 2 $\text{Gr}(13,4)$	$\text{Gr}(26,6)$ split into 2 $\text{Gr}(13,6)$	$\text{Gr}(26,8)$ split into 2 $\text{Gr}(13,8)$	$\text{Gr}(26,10)$ split into 2 $\text{Gr}(13,10)$
$\text{Gr}(26,12)$ split into 2 $\text{Gr}(13,12)$	$\text{Gr}(27,2)$ split into 3 $\text{Gr}(9,2)$ or 9 $\text{Gr}(3,2)$	$\text{Gr}(27,4)$ split into 3 $\text{Gr}(9,4)$	$\text{Gr}(27,6)$ split into 3 $\text{Gr}(9,6)$	$\text{Gr}(27,8)$ split into 3 $\text{Gr}(9,8)$
$\text{Gr}(28,2)$ splits into 2 $\text{Gr}(14,2)$ or 4 $\text{Gr}(7,2)$ or 7 $\text{Gr}(4,2)$	$\text{Gr}(28,3)$ splits into 2 $\text{Gr}(14,3)$ or 7 $\text{Gr}(4,3)$	$\text{Gr}(28,4)$ split into 2 $\text{Gr}(14,4)$ or 4 $\text{Gr}(7,4)$	$\text{Gr}(28,5)$ split into 2 $\text{Gr}(14,5)$	$\text{Gr}(28,6)$ split into 2 $\text{Gr}(14,6)$ or 4 $\text{Gr}(7,6)$
$\text{Gr}(28,7)$ split into 2 $\text{Gr}(14,7)$	$\text{Gr}(28,8)$ split into 2 $\text{Gr}(14,8)$	$\text{Gr}(28,9)$ split into 2 $\text{Gr}(14,9)$	$\text{Gr}(28,10)$ split into 2 $\text{Gr}(14,10)$	$\text{Gr}(28,11)$ split into 2 $\text{Gr}(14,11)$
$\text{Gr}(28,12)$ split into 2 $\text{Gr}(14,12)$	$\text{Gr}(28,13)$ split into 2 $\text{Gr}(14,13)$	$\text{Gr}(30,2)$ split into 2 $\text{Gr}(15,2)$ or 3 $\text{Gr}(10,2)$ or 5 $\text{Gr}(6,2)$ or 6 $\text{Gr}(5,2)$ or 10 $\text{Gr}(3,2)$	$\text{Gr}(30,3)$ split into 3 $\text{Gr}(10,3)$ or 5 $\text{Gr}(6,3)$	$\text{Gr}(30,4)$ split into 2 $\text{Gr}(15,4)$ or 3 $\text{Gr}(10,4)$ or 5 $\text{Gr}(6,4)$ or 6 $\text{Gr}(5,4)$
$\text{Gr}(30,5)$ split into 3 $\text{Gr}(10,5)$ or 5 $\text{Gr}(6,5)$	$\text{Gr}(30,6)$ split into 2 $\text{Gr}(15,6)$ or 3 $\text{Gr}(10,6)$	$\text{Gr}(30,7)$ split into 3 $\text{Gr}(10,7)$	$\text{Gr}(30,8)$ split into 2 $\text{Gr}(15,8)$ or $\text{Gr}(10,8)$	$\text{Gr}(30,9)$ split into 3 $\text{Gr}(10,9)$
$\text{Gr}(30,10)$ split into 2 $\text{Gr}(15,10)$	$\text{Gr}(30,12)$ split into 2 $\text{Gr}(15,12)$	$\text{Gr}(30,14)$ split into 2 $\text{Gr}(15,14)$		

<sup>a</sup>Graphs which cannot be split into connected subgraphs are not shown.

saddle points connecting these minima have  $C_{2v}$  symmetry (with the  $\text{Li}^+$  cation coordinated to an edge of the  $\text{BH}_4^-$  tetrahedron). Therefore from every global minima, there exist three paths leading to three saddle points, so the order of each vertex is three. The FPI group of this molecule is  $G^{(48)}$  and can be written as a direct product of  $S_4 \otimes S_1 \otimes S_1 \otimes \epsilon$ . The order of this group is 48, and the order of the minimum-energy structure's  $C_{3v}$  point group is 6. Therefore this molecule has  $48/6=8$  global minima on its PES. Because the symmetry of the saddle points is  $C_{2v}$  (order 4), the number of saddle points is  $48/4=12$ . *Ab initio* studies of this molecule have shown only the  $\text{Li}^+$

cation movement around  $\text{BH}_4^-$  to be flexible, while interconversion of the tetrahedral anion's H atoms are forbidden by high barriers.<sup>16</sup> Therefore, the FPI group of this molecule is *not* the proper group to use, and the  $\text{Gr}(8,3)$  graph is hence, not proper to use either.

The graph of this molecule which takes into account only the nonrigid movement of  $\text{Li}^+$  around the quasirigid  $\text{BH}_4^-$  anion is presented in Fig. 2.<sup>16</sup> We see that this graph consists of two equivalent subgraphs  $\text{Gr}(4,3)$ , consistent with the predictions of Table III which shows that  $\text{Gr}(8,3)$  can split into two  $\text{Gr}(4,3)$  graphs. Because all operations that involve inversion of all nuclei are forbidden by large

energy barriers, the rovibrational levels of flexible molecules of this type should be classified according to  $G^{(24)}$ , which is isomorphic to the  $T_d$  point group. While such splittings have not yet been observed experimentally, they have been predicted on the basis of numerical nonrigid Hamiltonian calculations.<sup>17</sup>

Trial calculations of the nonrigid vibrational levels of  $\text{LiBH}_4$ ,  $\text{NaBH}_4$ , and  $\text{LiCH}_4^+$  with nonrigidity belonging to the subgraph  $\text{Gr}(4,3)$  (i.e.,  $N_1=4$ ,  $v=3$ ) have been performed by Baranov and Boldyrev.<sup>17</sup> In their calculations, a simple two-dimensional nonrigid model describes the  $\text{L}^+$  cation's internal rotation around  $\text{BH}_4^-$  or  $\text{CH}_4$  with a fixed  $\text{L}^+-\text{MH}_4$  radius. The analytical potential energy surface used for these studies had minima, saddle points, and maxima with the  $\text{L}^+$  ion located at the centers of tetrahedral faces, at the middle of the edges, and at the apices of the tetrahedron  $\text{MH}_4$ , respectively. The energy surface parameters for this model were taken from *ab initio* calculations. Recently, Ohashi and Hougen<sup>18</sup> and Hirota<sup>19</sup> considered the internal motion in  $\text{LMX}_4$  species from a more general point of view.

The eigenstates of these molecules computed in this model cannot be classified in accordance to the  $C_{3v}$  local symmetry of the global minima, because tunneling between the wells splits the states into components that correspond to flexible symmetry group  $G^{(24)}$  (or  $T_d$ ). The calculated tunneling splittings increase rapidly when moving from the lowest states to higher states. Near and above the energy of the saddle point, the tunneling splittings become comparable to the transition frequencies, as result of which these levels may be described only in accordance with the nonrigid symmetry  $G^{(24)}$ .

The correspondence between the three representations of the  $C_{3v}$  group and those for  $T_d$  are as follows:

$$A_1 \rightarrow A_1 + T_2,$$

$$A_2 \rightarrow A_2 + T_1,$$

$$E \rightarrow E + T_1 + T_2.$$

The calculated vibrational energy levels in Ref. 17 did indeed follow patterns and degeneracy that should be for these symmetry labels.

While  $\text{LiBH}_4$  [Refs. 10(b) and 10(c)] and  $\text{NaBH}_4$  [Refs. 10(a) and 10(c)] have been studied in gas phase microwave spectra, the predicted tunneling splittings were not observed for either of these molecules. Hirota and co-workers<sup>10(b)</sup> pointed out that the tunneling barriers used in the dynamics calculations were too low (according to more sophisticated *ab initio* calculations, these barriers should be 1.5–2.0 times as high as those used). This could then explain why these splittings were not observed in the microwave experiments. However, for *excited* vibrational states of  $\text{LiBH}_4$ ,  $\text{NaBH}_4$  or  $\text{LiCH}_4^+$  as well as for similar molecules with lower barriers (e.g.,  $\text{LiAlH}_4$  and  $\text{NaAlH}_4$ ), such splittings may indeed be observed.

Other examples with PES described by disconnected graphs are  $\text{CH}_4^+$  and  $\text{BH}_4$ , which are Jahn–Teller unstable species. The local symmetry of the global minima are  $C_{2v}$  for both according to the best theoretical calculations<sup>20</sup> and

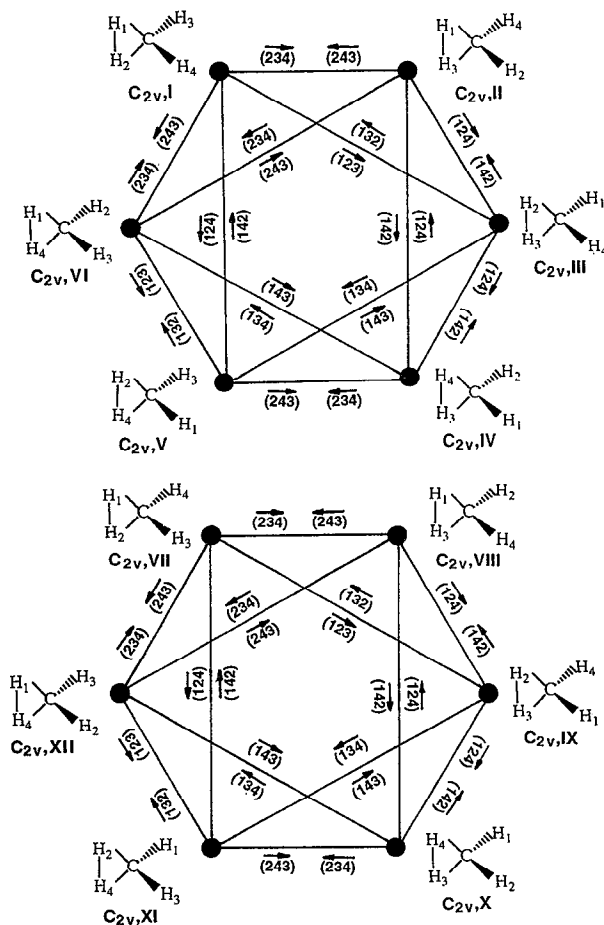


FIG. 4. Graph representing the nonrigid intramolecular rearrangement of the  $\text{CH}_4^+$  and  $\text{BH}_4$  molecules.

to experimental studies.<sup>21</sup> However, the barriers for the intramolecular rearrangements from one minimum to another, through local-symmetry  $C_s$  transition states, are not high (ca. 1 kcal/mol for  $\text{CH}_4^+$ ,<sup>20(a),20(c)</sup> and 7 kcal/mol for  $\text{BH}_4$ ,<sup>20(d)</sup> including ZPE correction).

The FPI group of the  $\text{CH}_4^+$  cation and  $\text{BH}_4$  cation and  $\text{BH}_4$  molecule is the direct product of the permutation group  $S_4$  (permutations of protons),  $S_1$  (permutations of carbon or boron), and inversion:  $S_4 \otimes S_1 \otimes \epsilon$ . The order of this group is  $4! \times 1! \times 2 = 48$ . According to the rules given in Sec. III, the number of global minima is  $48$  (order of the FPI group)/ $4$  (order of the  $C_{2v}$  group) =  $12$ , and the number of saddle points is  $48$  (order of FPI group)/ $2$  (order of the  $C_s$  group) =  $24$ . From every  $C_{2v}$  global minimum, four minimal energy paths lead to other global minima through  $C_s$  symmetry saddle points. According to *ab initio* calculations, there are two types of saddle points of  $C_s$  symmetry. The lower energy pathways proceed via transition structures of  $C_s$  symmetry which connect minima with the same chirality. Therefore, if we consider only rearrangements with the lowest barriers, the resulting graph of the intramolecular rearrangements has the form presented in

TABLE IV. Table of characters of the nonrigid  $G^{(24)}$  group of the  $\text{LiBH}_4$  molecule.

$G^{(24)}$	$E$	(123)	(12)	(1234)	(12)(34)
Order	1	8	6	6	3
$A_1$	1	1	1	1	1
$A_2$	1	1	-1	-1	1
$E$	2	-1	0	0	2
$T_1$	3	0	-1	1	-1
$T_2$	3	0	1	-1	-1

Fig. 4 which appeared in an article by Paddon-Row *et al.*<sup>20(a)</sup> The flexible group describing delocalization of such a molecule through six global minima according to the subgraph  $\text{Gr}(6,4)$  may be found by starting from the  $C_{2v}$  local symmetry group and multiplying by permutation-inversion elements that connect one global minima to another. The resulting nonrigid group  $G^{(24)}$  has 24 elements and its table of characters is presented in Table IV. This group is isomorphic to the  $T_h$  point group.<sup>22</sup> The order of  $G^{(24)}$  is half that of the FPI group because we assumed that moving from minima with  $S$  chirality to minima with  $R$  chirality is forbidden by large barriers.

In the above example, we have a graph that is not of the  $\text{Gr}(n,2)$  or  $\text{Gr}(n,n-1)$  families. This is a case where the group of the graph  $\text{Gr}(6,4)$  does not describe the nonrigid symmetry of the  $\text{CH}_4^+$  or  $\text{BH}_4$  molecule. In summary, when high energy barriers make some of the interconversions of  $n$  global minima impossible, the FPI group  $\text{Gr}(n,v)$  is inappropriate. The  $\text{Gr}(n,v)$  graph must be split into  $k$  subgraphs  $\text{Gr}(n_1,v)$  after which the nonrigid group obtained from the  $\text{Gr}(n_1,v)$  graph can be used to label the vibration/rotation energy levels of the molecule.

## V. SUMMARY

In this paper we have shown how permutation-inversion symmetry can be used to label the vibration/rotation wave functions and energy levels of floppy molecules. More rigid species undergo simple, nearly harmonic

TABLE V. Table of characters of the nonrigid  $G^{(24)}$  group of the  $\text{CH}_4^+$  cation. [ $\epsilon$  is  $\exp(2\pi i/3)$ .]

	$E$	(123)	(234)	(12)(34)	$E^*$	(123)*	(234)*	(12)(34)*
Order	1	4	4	3	1	4	4	3
$A_g$	1	1	1	1	1	1	1	1
$E_g$	1	$\epsilon$	$\epsilon^*$	1	1	$\epsilon$	$\epsilon^*$	1
$E_g^*$	1	$\epsilon^*$	$\epsilon$	1	1	$\epsilon^*$	$\epsilon$	1
$T_g$	3	0	0	-1	3	0	0	-1
$A_u$	1	1	1	1	-1	-1	-1	-1
$E_u$	1	$\epsilon$	$\epsilon^*$	1	-1	$-\epsilon$	$-\epsilon^*$	-1
$E_u^*$	1	$\epsilon^*$	$\epsilon$	1	-1	$-\epsilon^*$	$-\epsilon$	-1
$T_u$	3	0	0	-1	-3	0	0	1

vibrational motion about a global or local minimum on their potential energy surfaces. In these cases, the point group symmetry of the minimum-energy geometry can be used. Floppy molecules' energy levels *cannot* be labeled by the point group symmetries of any one of their minimum-energy geometries because their vibrational wave functions may sample numerous such minima.

Our development is based on describing the potential energy surface of a floppy molecule in terms of  $n$ , the number of equivalent *global* minima, as well as  $v$ , the number of *other* global minima which can be reached via energetically accessible paths from any one minimum. A graph with  $n$  vertices and  $v$  lines connecting each vertex to  $v$  other vertices is used to generate the permutation-inversion symmetry group required to label the vibration/rotation energy levels of the molecule. The  $\text{ArH}_3^+$  and  $\text{C}_2\text{H}_3^+$  cations are used as illustrative examples.

In species such as  $\text{Li}^+\text{BH}_4^-$  and  $\text{CH}_4^+$  not all of the global minima can be interconverted via energetically accessible paths. In such cases, the graph connecting the  $n$  minima *splits* into two or more equivalent subgraphs each describing energetically accessible interconversions among subsets of the  $n$  minima. The permutation-inversion group obtained according to these subgraphs can be used to label the vibration/rotation energy levels in these cases. Table III lists, for species having 6 to 30 minimum-energy structures, how graphs for  $n$  minima can split into  $k$  subgraphs for the sets of  $n/k$  minima that are interconvertible.

## ACKNOWLEDGMENT

This work was supported by the National Science Foundation, Grant No. CHE9116286.

- H. C. Longuet-Higgins, *Mol. Phys.* **3**, 445 (1963).
- P. R. Bunker, *Molecular Symmetry and Spectroscopy* (Academic, New York, 1979).
- H. Frei, A. Bauer, and H. H. Guthard, *Top. Current Chem.* **81**, 1 (1979).
- G. S. Ezra, *Symmetry Properties of Molecules. Lecture Notes in Chemistry* (Springer, Berlin, 1982), Vol. 28.
- Y. G. Smeyers and A. Hernandez-Laguna, in *Structure and Dynamics of Molecular Systems*, edited by R. Daudel *et al.* (Reidel, Dordrecht, 1985), pp. 23-40.
- T. J. Lee and H. F. Schaefer III, *J. Chem. Phys.* **85**, 3437 (1986); J. A. Pople, *Chem. Phys. Lett.* **137**, 10 (1987); R. Lindh, R. O. Roos, and W. P. Kremer, *ibid.* **139**, 407 (1987); C. Liang, T. P. Hamilton, and H. F. Schaefer III, *J. Chem. Phys.* **92**, 3653 (1990).
- J. T. Hougen, *J. Mol. Spectrosc.* **123**, 197 (1987); R. Escibano, P. R. Bunker, and P. C. Gomes, *Chem. Phys. Lett.* **150**, 6; (1988); P. C. Gomes and P. R. Bunker, *ibid.* **165**, 351 (1990).
- M. W. Crofton, M. F. Jagod, B. D. Rehffuss, and T. Oka, *J. Chem. Phys.* **91**, 5139 (1989).
- A. I. Boldyrev, O. P. Charkin, N. G. Rambidi, and V. I. Avdeev, *Chem. Phys.* **44**, 20 (1976); J. D. Dill, P. v. R. Schleyer, J. S. Binkley, and J. A. Pople, *J. Am. Chem. Soc.* **99**, 6159 (1977).
- (a) Y. Kawashima, C. Yamada, and E. Hirota, *J. Chem. Phys.* **94**, 7707 (1991); (b) Y. Kawashima and E. Hirota, *ibid.* **96**, 2460 (1992); (c) J. Mol. Spectrosc. **153**, 466 (1992).
- V. L. Pershin and A. I. Boldyrev, *J. Mol. Struct. (THEOCHEM)* **150**, 171 (1987).
- A. I. Boldyrev, in *Modern Problems of Physical Chemistry*, edited by Ya. M. Kolotyrykin (Khimia, Moscow, 1988), Chap. I, pp. 6-47.
- F. Harary, *Graph Theory* (Addison-Wesley, Reading, 1969).
- (a) E. D. Simandiras, J. F. Gaw, and N. C. Handy, *Chem. Phys. Lett.* **141**, 166 (1987); (b) R. Escibano and P. R. Bunker, *J. Chem. Phys.*

- 88, 4120 (1988); (c) M. Bogey, H. Bolvin, C. Demuynck, and J. L. Destombes, *Phys. Rev. Lett.* **58**, 988 (1987); (d) *J. Chem. Phys.* **88**, 4120 (1988).
- <sup>15</sup> Yu. B. Kirrilov, A. I. Boldyrev, N. M. Klimenko, and O. P. Charkin, *Koord. Khim.* **8**, 1203 (1982); Yu. B. Kirrilov and A. I. Boldyrev, *Dokl. Akad. Nauk SSSR* **272**, 635 (1983).
- <sup>16</sup> A. I. Boldyrev, in *Structure and Dynamics of Non-Rigid Systems*, edited by Yves G. Smeyers (Kluwer Academic, Dordrecht, 1993).
- <sup>17</sup> L. Ya. Baranov and A. I. Boldyrev, *Chem. Phys. Lett.* **96**, 218 (1983).
- <sup>18</sup> N. Ohashi and J. T. Hougen, *J. Mol. Spectrosc.* **153**, 429 (1992).
- <sup>19</sup> E. Hirota, *J. Mol. Spectrosc.* **153**, 447 (1992).
- <sup>20</sup> (a) M. N. Paddon-Row, D. J. Fox, J. A. Pople, K. N. Houk, and D. W. Pratt, *J. Am. Chem. Soc.* **107**, 7696 (1985); (b) K. Takeshita, *J. Chem. Phys.* **86**, 329 (1985); (c) R. F. Frey and E. R. Davidson, *ibid.* **88**, 1775 (1988); (d) M. N. Paddon-Row and S. S. Wong, *J. Mol. Struct. (Theochem)* **180**, 353 (1988).
- <sup>21</sup> (a) L. B. Knight, Jr., J. Steadman, D. Feller, and E. R. Davidson, *J. Am. Chem. Soc.* **106**, 3700 (1984); (b) M. C. R. Symons, T. Chen, and C. Glidewell, *J. Chem. Soc. Chem. Commun.* **326** (1983); (c) T. A. Claxton, T. Chen, M. C. R. Symons, and C. Glidewell, *Faraday Discuss. Chem. Soc.* **78**, 121 (1984).
- <sup>22</sup> Our table of characters of the  $T_h$  group is somewhat different from that published in, for example, F. A. Cotton, *Chemical Applications of Group Theory*, 3rd ed. (Wiley, New York, 1990); A. Vincent, *Molecular Symmetry and Group Theory* (Wiley, Chichester, 1977), which are incorrect in their characters for the inversion operation of triply degenerate representations.